Exact Parameter Determination for Parkinson's Disease Diagnosis with PET Using an Algebraic Approach

Hiroshi Yoshida[1], Koji Nakagawa[2], Hirokazu Anai[3], and Katsuhisa Horimoto[2]

[1] Faculty of Mathematics, Organization for the Promotion of Advanced Research, Kyushu University, Hakozaki 6-10-1, Higashi-ku, Fukuoka 812-8581 Japan
phiroshi@math.kyushu-u.ac.jp
[2] Computational Biology Research Centre (CBRC), National Institute of Advanced Industrial Science and Technology (AIST), Aomi 2-42, Koto-ku, Tokyo 135-0064, Japan
{nakagawa-koji,k.horimoto}@aist.go.jp
[3] IT Core Laboratories, FUJITSU LABORATORIES LTD./CREST, JST., Kamikodanaka 4-1-1, Nakahara-ku, Kawasaki 211-8588, Japan
anai@jp.fujitsu.com

Abstract. The mechanism of Parkinson's disease can be investigated at the molecular level by using radio-tracers. The concentration of dopamine in the brain can be observed by using a radio-tracer, 6-[^{18}F]fluorodopa (FDOPA), with positron emission tomography (PET), and the dopamine kinetics can be described as compartmental models for tissues of the brain. The models for FDOPA kinetics are solved explicitly, but the solution shows a complicated form including several convolutions over time domain. Owing to the complicated form of the solution, graphical analyses such as Logan or Patlak analysis have been utilized as conventional methods over past decades. Because some kinetic constants for Parkinson's disease are estimated in the graphical analyses with the slope or intercept of the line obtained under various assumptions, only a limited set of parameters have approximately been estimated. We have analysed the compartmental models by using the Laplace transformation of differential equations and by algebraic computation with the aid of Gröbner base constructions. We have obtained a rigorous solution with respect to the kinetic constants over the Laplace domain. Here, we first derive a rigorous solution for the parameters, together with a discussion about the merits of the derivation. Next, we describe a procedure to determine the kinetic constants with the observed time–radioactivity curves. Last, we discuss the feasibility of our method, especially as a criterion for diagnosing Parkinson's disease.

1 Introduction

Radio-tracers are often used to analyse metabolic systems in biomedical research. Usually the kinetics of metabolism are described as compartmental models, and kinetic constants are numerically estimated using the measurement of radio-tracers to diagnose the disease. In particular, the positron emission tomography (PET) has been developed to measure the details of metabolic events hitherto unavailable, and is especially useful to determine the kinetic constants to assist the diagnosis of various diseases.

H. Anai, K. Horimoto, and T. Kutsia (Eds.): AB 2007, LNCS 4545, pp. 110–124, 2007.
© Springer-Verlag Berlin Heidelberg 2007

Parkinson's disease, which is due to abnormal levels of dopamine in the brain, is one of the diseases that can be diagnosed by radio-tracer measurement with PET, and by determination of kinetic constants in compartmental models for plasma and brain tissue [12]. There are two approaches to measuring the activity of radio-tracers. One is a combination of the measurement of a radio-tracer, L-3,4-dihydroxy-6-[^{18}F]fluoro-phenylalanine (FDOPA) in the brain, and sampling the blood to measure the total activity of FDOPA (approach with blood sampling), and the other is the measurement of the FDOPA activity in two brain tissues (approach without blood sampling). In both approaches, the kinetics can be described as sets of compartmental models. Fortunately, a system of differential equations in the two sets of models can be solved explicitly , but unfortunately the solutions for estimating the kinetic constants are highly complicated. Indeed, the solutions are expressed by a few convolutions of complicated equations.

To overcome analytical difficulties in determining kinetic constants, there are two conventional methods of kinetic constant estimation in the compartmental models, Patlak Analysis [18, 19] and Logan Analysis [15]. In both methods, the combination of some parameters with various approximations is assumed to form a straight line as metabolism approaches an equilibrium. By plotting the observed data around the metabolic equilibrium (graphical analysis), the combined parameters can be estimated using the slope or intercept in the plotted line [14, 18].

By using graphical analysis, Parkinson's disease has been extensively studied in the two approaches with and without the blood sampling. In the approach using blood sampling, the kinetic constants with respect to plasma are calculated from the blood-sampling data, and then, using these constants, measurements for Parkinson's disease such as the constants describing FDOPA kinetics in brain tissue are calculated [10, 11, 12, 20]. In addition, Martin et al. [16] considered L-3,4-dihydroxy-6-[^{18}F]fluoro-3-O-methylphenylalanine (3-OMFD) in compartmental models for FDOPA metabolism, because FDOPA is converted to 3-OMFD [1, 17], which has an influence on the total radioactivity observed in plasma and in the brain tissue by crossing the blood-brain barrier (BBB). In an approach without blood sampling, using the time–radioactivity curves of two distinct brain tissues, the constants for Parkinson's disease diagnosis are calculated [9, 14].

The diagnosis of Parkinson's disease with PET depends on graphical analysis, a simple presentation of the relationships between the kinetic constants of the FDOPA kinetics. However, the present analyses require further improvement for precise diagnoses. For example, graphical analysis using blood sampling is cumbersome, partly because the sampling requires a load to the patients, and partly because the separate measurement of radio-tracer from the blood provides an obstacle for the precise estimation of parameters such as the time delay and contamination of the samples in the tubing. Graphical analysis without blood sampling produces a highly complicated model and therefore requires various assumptions and approximations to estimate kinetic constants. Thus, the choice between the two approaches involves a trade-off between cumbersome blood sampling and difficult efficient parameter determination. Indeed, by considering the pitfalls described above, some methods have also designed by using different radio-tracers. For instance, Ichise et al. [8] proposed a method without blood sampling by using [^{123}I]iodobenzofuran, and Lammertsma et al. [13] and

Logan et al. [14] proposed a method without blood sampling by using [^{11}C]raclopride, in which the cerebellum or cerebral cortex was used as a reference tissue and analysed as a single-tissue compartment. Although the pitfalls have partially been overcome, a rigorous solution has not yet been analysed.

In this paper, we propose radical deliverance from the aforementioned difficulty. We present an efficient method for determining kinetic constants for FDOPA kinetics with PET using an algebraic approach. The compartmental models are rigorously solved by the Laplace transformation of differential equations into algebraic equations, and by the following symbolic computation with the aid of Gröbner bases. Such usage of symbolic computation has overcome the analytical difficulties in the previous study [6], where general theory of compartmental models was derived over the Laplace domain for PET, but the analysis or determination of kinetic constants still required the system's equilibrium or steady state. In our method, by contrast, the derivation of a relationship between the observed concentrations without blood sampling by PET does not need any approximations and assumptions for the kinetic constants. Here, we first derive rigorous relationships between the parameters, and we discuss the merits of the derivation, in comparison with graphical analyses. Second, we describe an efficient procedure for determining the kinetic constants with observed time–radioactivity curves. Last, we discuss the feasibility of our method, especially as a criterion for diagnosing Parkinson's disease.

2 Model and Method

In this section, we introduce three compartmental models to describe the metabolism of the radio-tracer FDOPA and its metabolites with respect to two brain tissues and plasma. Differential equations corresponding to the kinetic model are derived, and the equations are transformed into a system of algebraic equations. Surprisingly, the rigorous solution is of a simple form over the Laplace domain. Finally, we describe a procedure to determine the kinetic constants of the models, which is performed over the Laplace domain.

2.1 Compartmental Model

Compartmental models (A) and (B) are introduced for the radio-tracer FDOPA and its metabolite 3-OMFD as shown in Figs. 1 (a) and (b). For simplicity, let A- and B-tissues denote tissues in which the radio-tracer kinetics can be described as shown in Figs. 1 (a) and (b), respectively. In the actual brain, A- and B-tissues correspond to the striatum (putamen/caudate) and the cerebellum/cerebral cortex in the brain [4, 7]. Furthermore, it is assumed that the relationships between plasma FDOPA, 3-OMFD, and extra-vascular 3-OMFD can be described as the compartmental model (C) as shown in Fig. 1 (c).

2.2 Kinetic Equations

According to the kinetic model in Fig. 1, the following system of differential equations has been obtained:

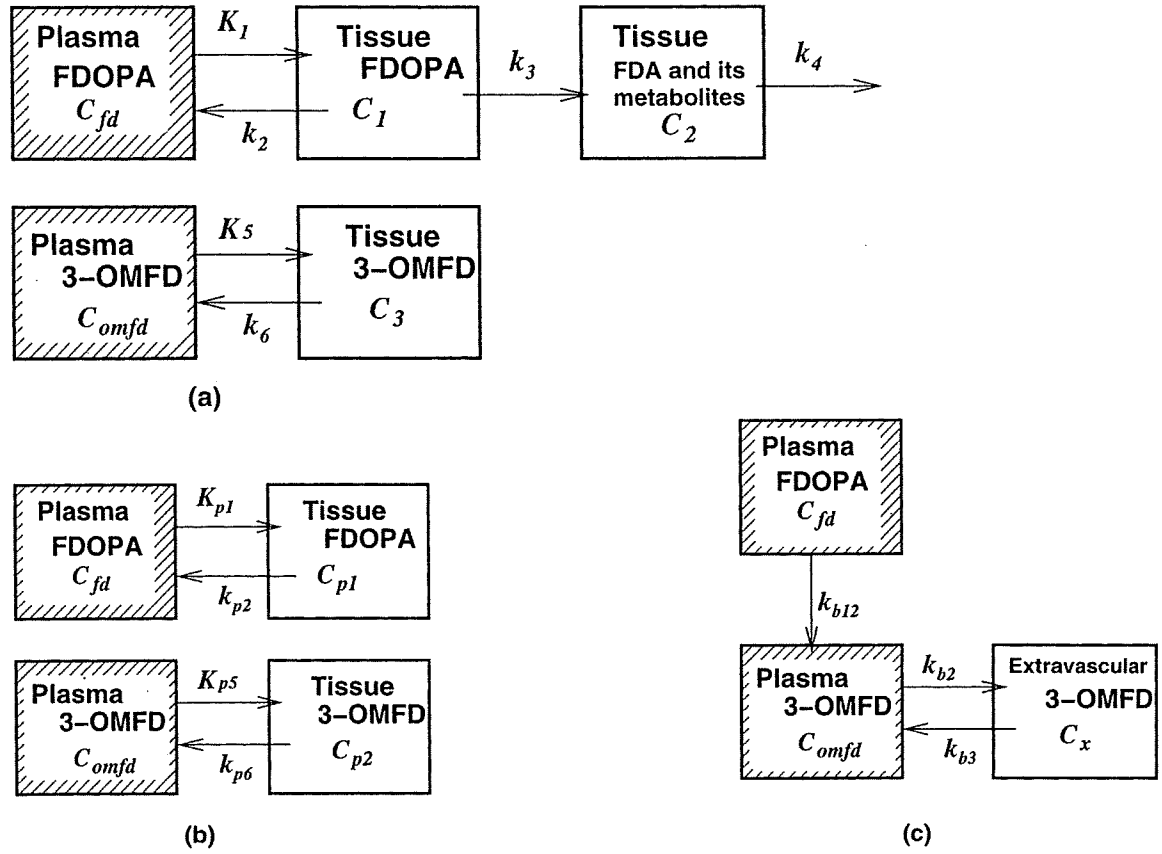

Fig. 1. Compartmental models for describing the radio-tracer kinetics in this paper, which were originally introduced by Huang et al. [7]. The shaded boxes represent the kinetics in plasma. (a) Model for A-tissue. Three separate compartments for tissue FDOPA, tissue FDA (and its metabolites), and tissue 3-OMFD. (b) Model for B-tissue which is the same as (a), except that there is no compartment for FDA. (c) Model for plasma FDOPA to 3-OMFD in the periphery of one compartment for plasma 3-OMFD and one for the extra-vascular pool.

Time (A-Tissue)

$$\begin{cases} \dfrac{dC_1}{dt} = K_1 C_{fd}(t-\tau)\theta(t-\tau) - (k_2+k_3)C_1, \\ \dfrac{dC_2}{dt} = k_3 C_1 - k_4 C_2, \\ \dfrac{dC_3}{dt} = K_5 C_{omfd}(t-\tau)\theta(t-\tau) - k_6 C_3, \end{cases} \tag{1}$$

Time (B-Tissue)

$$\begin{cases} \dfrac{dC_{p1}}{dt} = K_{p1} C_{fd}(t-\tau)\theta(t-\tau) - k_{p2} C_{p1}, \\ \dfrac{dC_{p2}}{dt} = K_{p5} C_{omfd}(t-\tau)\theta(t-\tau) - k_{p6} C_{p2}, \end{cases} \tag{2}$$

Time (C-Blood (Plasma))

$$\begin{cases} \dfrac{dC_{omfd}}{dt} = k_{b12}C_{fd} - k_{b2}C_{omfd} + k_{b3}C_x, \\ \dfrac{dC_x}{dt} = k_{b2}C_{omfd} - k_{b3}C_x. \end{cases} \tag{3}$$

In the compartmental model (A), (B), and (C), every one of the initial values is assumed to be zero because of non-existence of the radio-tracers and their metabolites at starting time $t = 0$. However, there exists the time delay τ of the observed blood curve (C) relative to tissue measurements (A) and (B). That is, τ designates a difference between the starting times of (A), (B), and (C). This effect leads to the terms $C_{fd}(t-\tau)\theta(t-\tau)$ and $C_{omfd}(t-\tau)\theta(t-\tau)$, where $\theta(t)$ is the unit step function defined as follows:

$$\theta(t) = \begin{cases} 0 & (t < 0), \\ 1 & (t > 0). \end{cases}$$

The differential equations describing the A- and B-tissues and the C-blood kinetics models can be changed into the following equations over the Laplace domain:

Laplace (A)

$$\begin{cases} sL[C_1] = K_1 e^{-s\tau}L[C_{fd}] - (k_2 + k_3)L[C_1], \\ sL[C_2] = k_3 L[C_1] - k_4 L[C_2], \\ sL[C_3] = K_5 e^{-s\tau}L[C_{omfd}] - k_6 L[C_3], \end{cases} \tag{4}$$

Laplace (B)

$$\begin{cases} sL[C_{p1}] = K_{p1} e^{-s\tau}L[C_{fd}] - k_{p2}L[C_{p1}], \\ sL[C_{p2}] = K_{p5} e^{-s\tau}L[C_{omfd}] - k_{p6}L[C_{p2}], \end{cases} \tag{5}$$

Laplace (C)

$$\begin{cases} sL[C_{omfd}] = k_{b12}L[C_{fd}] - k_{b2}L[C_{omfd}] + k_{b3}L[C_x], \\ sL[C_x] = k_{b2}L[C_{omfd}] - k_{b3}L[C_x], \end{cases} \tag{6}$$

where $L[f]$ denotes the Laplace transformation of f. Thus, a system of differential equations is transformed into a system of corresponding algebraic equations.

2.3 Rigorous Solution

In the approach without blood sampling, the data observed using PET scanning are limited to the total radioactivities: $Cs(t) = C_1(t) + C_2(t) + C_3(t)$ and $Cc(t) = C_{p1}(t) + C_{p2}(t)$. Let $Cs(s)$ and $Cc(s)$ denote the Laplace transformations of $Cs(t)$ and $Cc(t)$, respectively. Then, the solution to the system of algebraic equations of Laplace (A),

(B), and (C) has been obtained, leading to a rigorous and simple relationship between $Cs(s)$ and $Cc(s)$ as follows:

$$\frac{Cs(s)}{Cc(s)} = \frac{(s+k_{p2})(s+k_{p6})}{(s+k_2+k_3)(s+k_4)(s+k_6)} \times \frac{K_5 k_{b12}(s+k_2+k_3)(s+k_4)(s+k_{b3}) + sK_1(s+k_3+k_4)(s+k_6)(s+k_{b2}+k_{b3})}{K_{p5}k_{b12}(s+k_{b3})(s+k_{p2}) + sK_{p1}(s+k_{b2}+k_{b3})(s+k_{p6})}. \tag{7}$$

Thus, $Cs(s)/Cc(s)$ is a rational function in s to which symbolic methods such as Gröbner base computations can be applied, resulting in exact and efficient parameter determination.

2.4 Procedure to Determine the Kinetic Constants

Procedure overview. Fig. 2 shows an overview of the present procedure for determining the kinetic constants from radio-tracer activity data. The procedure is composed of two parts. First, we fit the observed radioactivity curves by a series of exponentials, and then the fitted series of exponentials are transformed into the corresponding algebraic equations by the Laplace transformation. Second, the kinetic constants in the rigorous equation (7) are determined using an algebraic approach. The details of the above procedure are described below.

Laplace transformation of the observed data. We need a Laplace transformation of the observed data because we perform parameter determination over the Laplace domain. Let $Cso(t)$ and $Cco(t)$ denote the observed data in A- and B-tissues, respectively. By using non-linear regression, $Cso(t)$ and $Cco(t)$ are expressed in terms of a series of exponentials according to [3] as follows:

$$\begin{cases} Cso(t) = & a_1 \exp(-m_1 t) + a_2 \exp(-m_2 t) - (a_1 + a_2 + aa)\exp(-m_3 t) + aa, \\ Cco(t) = & b_1 \exp(-l_1 t) + b_2 \exp(-l_2 t) - (b_1 + b_2 + bb)\exp(-l_3 t) + bb, \end{cases} \tag{8}$$

where the initial values are assumed to be zero, namely $Cso(0) = 0$ and $Cco(0) = 0$ because of non-existence of radio-tracer at $t = 0$ as mentioned in §2.2. However, this assumption has an inference on regression of the parameters: a_i, b_i, aa, bb, m_i and l_i owing to inaccuracy or noise in the observed data that leads to $Cso(0) \neq 0$ or $Cco(0) \neq 0$. To avoid this inference, we have adopted an additional value: η. We have firstly fitted the observed data with $Cso(t-\eta)$ and $Cco(t-\eta)$, and then have substituted η with 0, that is, η has been ignored. $Cso(t)$ and $Cco(t)$ thus fitted are changed into the Laplace-transformed data as follows:

$$\begin{cases} L[Cso(t)] = & \dfrac{a_1}{s+m_1} + \dfrac{a_2}{s+m_2} - \dfrac{a_1+a_2+aa}{s+m_3} + \dfrac{aa}{s}, \\ L[Cco(t)] = & \dfrac{b_1}{s+l_1} + \dfrac{b_2}{s+l_2} - \dfrac{b_1+b_2+bb}{s+l_3} + \dfrac{bb}{s}, \end{cases} \tag{9}$$

where L denotes the Laplace transformation.

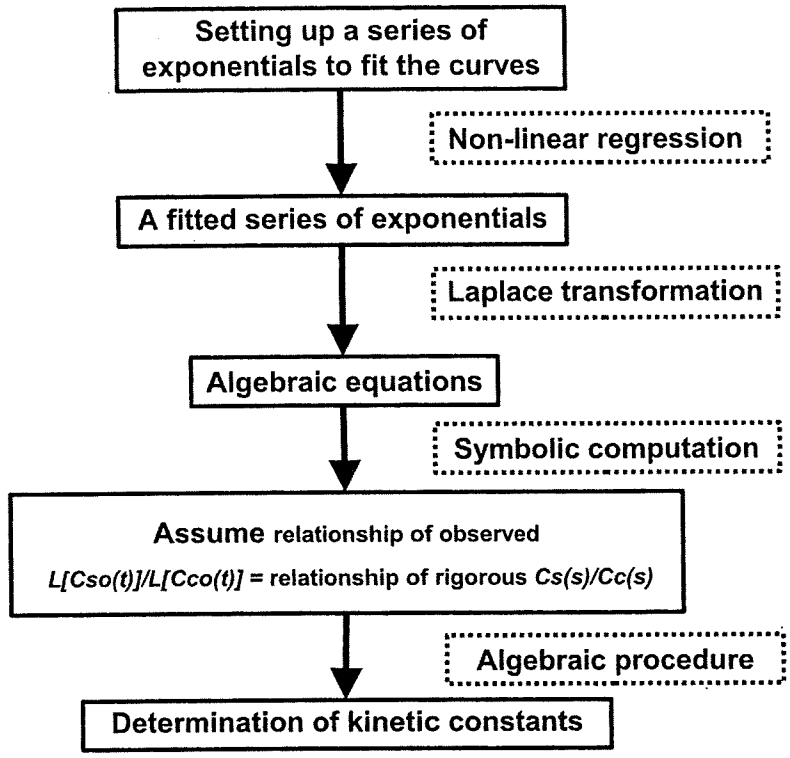

Fig. 2. Overview of the procedure for determining kinetic constants

Algebraic procedure. Without any error, the transformed function of A-tissue data, $L[Cso(t)](s)$, and that of B-tissue data, $L[Cco(t)]$, would be identical with $Cs(s)$ and $Cc(s)$, respectively. This fact has led us to the following procedure to determine the parameters over the Laplace domain.

1. $L[Cso(t)]/L[Cco(t)]$ can be transformed into the form: $F(s)/G(s)$, where $F(s)$ and $G(s)$ are both fifth-order polynomials in s. It follows from Eq. (7) that $-(k_2 + k_3)$, $-k_4$, and $-k_6$ are three of the real roots of $G(s)$. Likewise, $-k_{p2}$ and $-k_{p6}$ are two of the real roots of $F(s)$. It can be proved that both $F(s)$ and $G(s)$ have five real negative roots in PET experiments as mentioned in Appendix A.
2. Let $-r_i$ $(1 \leq i \leq 5)$ and $-t_i$ $(1 \leq i \leq 5)$ denote the real roots of $F(s)$ and $G(s)$, respectively. From (1), $k_2 + k_3$, k_4, and k_6 are three of t_i, e.g., t_1, t_2, and t_3. Likewise, k_{p2} and k_{p6} are, e.g., r_1 and r_2. The number of assignments of the parameters $k_2 + k_3, k_4, k_6, k_{p2}$, and k_{p6} to r_i and t_i is 1200. We apply these 1200 assignments to the two procedures below.
3. The remaining parameters, $K_1/K_{p1}, K_5k_{b12}/K_{p1}, K_{p5}k_{b12}/K_{p1}, k_2, k_3, k_{b2}$, and k_{b3}, are calculated by solving the following system of algebraic equations:

$$H(-r_3) = H(-r_4) = H(-r_5) = I(-t_4) = I(-t_5) = 0,\ k_2 + k_3 = t_1,$$
$$K_1/K_{p1} = HC(F(s))/HC(G(s)),$$

where $H(s) = K_5k_{b12}(s+k_2+k_3)(s+k_4)(s+k_{b3}) + sK_1(s+k_3+k_4)(s+k_6)(s+k_{b2}+k_{b3})$, $I(s) = K_{p5}k_{b12}(s + k_{b3})(s + k_{p2}) + sK_{p1}(s + k_{b2} + k_{b3})(s + k_{p6})$, and HC denotes the

head coefficient. To solve the system of algebraic equations above, we have derived the triangular form with the aid of Gröbner base computations. The third-order polynomial as the elimination ideal with respect to k_{b3} is shown in Appendix B.

4. Because the numerator and denominator of $Cs(s)/Cc(s)$ (Eq. (7)) are both sixth-order polynomials in s while $F(s)$ and $G(s)$ are both fifth-order, the similarity between $Cs(s)/Cc(s)$ and $F(s)/G(s)$ can be calculated by the difference between the roots of the numerator and denominator of $Cs(s)/Cc(s)$ that do not appear as the roots of $F(s)$ or $G(s)$. These two roots are calculated by coefficient comparison as follows:

$$k_3+k_4+k_6+k_{b2}+k_{b3}+K_5k_{b12}/K_1-(r_3+r_4+r_5),\ k_{b2}+k_{b3}+k_{p6}+K_{p5}k_{b12}/K_{p1}-(t_4+t_5).$$

We record the difference between the above two roots as *diff*. Notice that the roots of $F(s)$ and $G(s)$ correspond to the reciprocals of time constants of PET experiments and that they are distinct from one another.

5. The parameter sets determined above are arranged in ascending order by *diff*. Furthermore, we remove parameter sets that violate an empirical or physiological law. In this paper, we have adopted the following law:

$$k_{p2} < k_{p6} \text{ and } k_3 < 1. \tag{10}$$

The first inequality, $k_{p2} < k_{p6}$, designates a different permeability of FDOPA and 3-OMFD, which cross the BBB (blood-brain barrier) [5, 7]. The second inequality, $k_3 < 1$, is the empirical law.

6. The result of the procedure above is the first parameter set among the sets in ascending order by *diff*.

Using the procedure described above, we can immediately and effectively determine the parameters such that all of them are consistent with PET experiments.

3 Results

We have extracted the observed data of A- and B-tissues from Cumming and Gjedde [4, p.52, Fig. 4], where A- and B-tissues correspond to the caudate and the cerebral (occipital) cortex, respectively. First, we have fitted the ^{18}F radioactivity data in A- and B- tissues of the normal control subject and the patient with Parkinson's disease (PD) as a series of exponentials according to $Cso(t-\eta_A)$ and $Cco(t-\eta_B)$ in Eq. (8). The parameters obtained, $a_i, b_i, aa, bb, m_i, l_i$, are represented in Table 1. Figure 3 shows the fitting of the observed data. As seen in Fig. 3, the estimated curves are fitted from control and PD patient samples.

By using the parameters in Table 1, we have obtained kinetic constants according to the algebraic procedure in §2.4. This calculation needed 15 seconds CPU time and 5.5 MBytes memory via Mathematica 5.2 (Wolfram Research, Inc.) with Intel(R) Xeon(R) CPU 2.33GHz. Table 2 shows almost all kinetic constants of the control and PD patient,

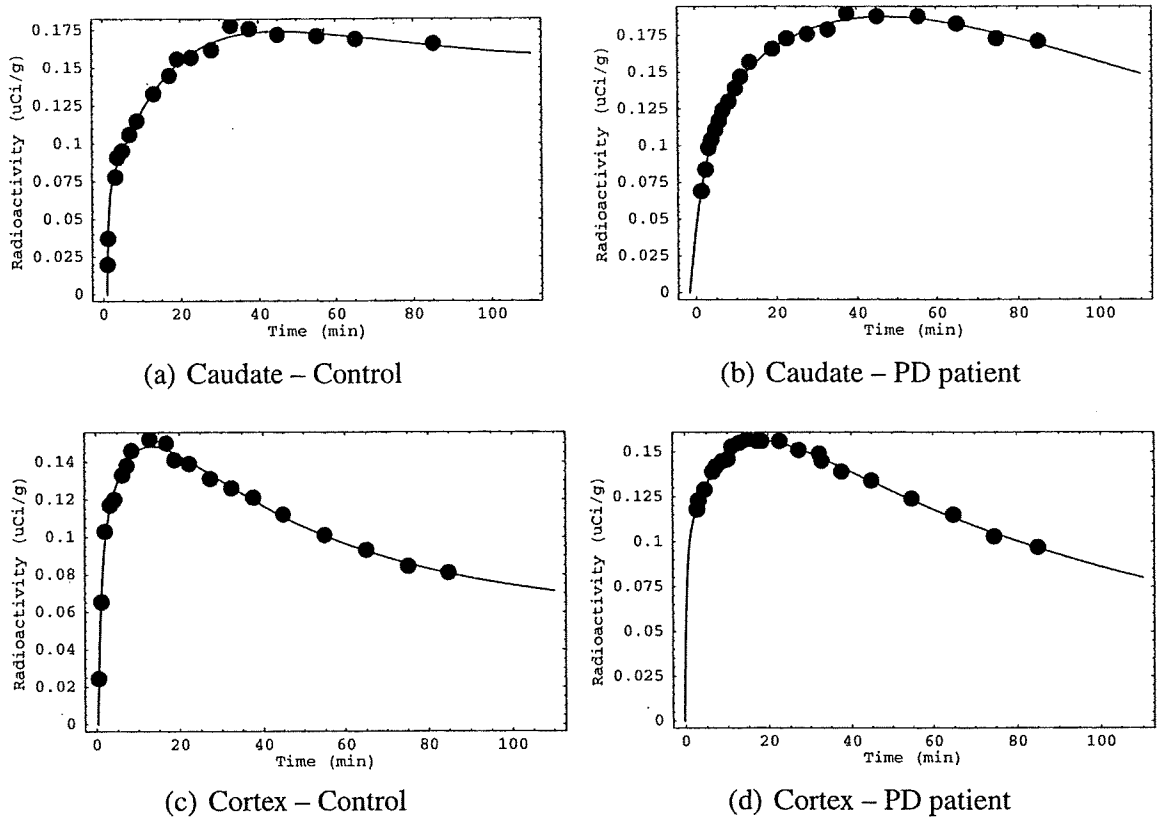

(a) Caudate – Control

(b) Caudate – PD patient

(c) Cortex – Control

(d) Cortex – PD patient

Fig. 3. Time–radioactivity curves in the occipital cortex and caudate of a patient with Parkinson's disease and a normal control subject during 90 min after administration of [^{18}F]fluorodopa. The circles are the observed data that have been extracted from [4, p.52, Fig. 4], and the solid curves are fits by a series of exponentials. (a) Radioactivity in caudate of a normal control subject. (b) Caudate of a patient with Parkinson's disease. (c) Occipital cortex of the control. (d) Occipital cortex of the patient.

in comparison with those in the previous estimation [4]. First, we have determined almost all values of kinetic constants, while the previous work only partially estimated the constants, using graphical analysis. Second, the orders of the kinetic constants obtained by our method are similar to those found by the graphical analysis, for both the control and PD patient. Interestingly, one constant, k_4, which is one of the measures for Parkinson's disease, was slightly different but consistent in our analysis compared with that in the previous study. The difference/consistency of the constants in the two studies will be judged from future work where many samples are analysed. At any rate, we have successfully determined almost all constants without blood-sampling data via our method.

4 Discussion

We have derived the equation Eq. (7), which enables us to determine rigorously almost all of the kinetic constants in the FDOPA model. In contrast, graphical analysis can only approximately determine the kinetic constants around the equilibrium of the

Table 1. The obtained parameters by non–linear regression

A-tissue ($Cso(t-\eta_A)$)	a_1	a_2	aa	m_1	m_2	m_3	η_A
Control	−0.0660074	−4.66107	0.153617	2.31191	0.0399169	0.038911	0.893464
PD patient	−0.10455	−3.02326	0.0588441	0.275661	0.0183807	0.0166495	−1.49546
B-tissue ($Cco(t-\eta_B)$)	b_1	b_2	bb	l_1	l_2	l_3	η_B
Control	−0.0826722	−0.11201	0.058033	1.31972	0.16269	0.021298	0.298255
PD patient	−0.0928105	−0.107709	0.0252521	2.05784	0.113904	0.0105398	−0.267787

Table 2. Kinetic constants of control and PD patient in FDOPA model by the procedure in §2.4 *without* blood–sampling data. The figures in the square bracket denote k_4 by Patlak analysis *with* blood–sampling data [4].

Kinetic constants	k_2	k_3	k_4	k_6	k_{p2}	k_{p6}	k_{b2}	k_{b3}
Control	0.0968	0.220	0.00674 [0.011 ± 0.003]	0.0389	0.0213	1.32	0.0525	0.00122
PD Patient	0.000818	0.0176	0.0166 [0.016 ± 0.004]	0.276	0.00231	0.0646	0.0276	0.112

(Continue)	K_1/K_{p1}	K_5k_{b12}/K_{p1}	$K_{p5}k_{b12}/K_{p1}$
Control	1.29	0.0466	0.979
PD Patient	0.165	0.291	0.120

system under various assumptions and ignorance [6]. For instance, even the striatum (corresponding to A-tissue in this paper) was modelled as a single-tissue compartment [9]. Moreover, replacement with averaged values and ignorance of error terms as a small value are required for the solution to the equation over time domain because of its complicated form. Thus, the present method by the algebraic approach has successfully overcome the difficulties of graphical analysis.

Apart from graphical analyses, Cobelli et al. [2, 3] have studied the relationship between the observational parameters and the unknown model parameters over the Laplace domain. The aim of these works was determination of a model in which, on the assumption that any noise does not exist, it is determined whether the parameters can be determined uniquely or non-uniquely. In contrast, in this paper, we have determined parameters from the observed data with noise via the algebraic procedure as mentioned in §2.4. One of the other procedures to determine parameters from noisy data is the least squares method. We have attempted the least squares method using the following equation:

$$\int_{ls}^{us} (Cs(s)L[Cco(t)](s) - Cc(s)L[Cso(t)](s))^2 \mathbf{d}s.$$

Although the selection of interval between ls and us is somewhat ambiguous and it takes about 2.7 hours for each simulation with AMD Opteron(tm) Processor 2.412GHz, this method usually brings us the same results as the algebraic procedure and might be suitable for the equation where blood vessels in tissues are taken into account.

The solution over the Laplace domain is an algebraic equation to which Gröbner base computations can be applied, resulting in a much simpler form and efficient parameter

determination (about 15 seconds with Intel(R) Xeon(R) CPU 2.33GHz). In fact, the equivalent equation to Eq. (7) can be described over time domain as follows:

$$\begin{aligned} Cs(t) &= Cc(t) \otimes Y_1(t) \otimes Y_2(t), \\ \text{with } Y_1(t) &= \frac{(k_2+k_3-k_{p2})(k_2+k_3-k_{p6})}{(k_2+k_3-k_4)(k_2+k_3-k_6)} e^{-(k_2+k_3)t} \\ &\quad - \frac{(k_4-k_{p2})(k_4-k_{p6})}{(k_2+k_3-k_4)(k_4-k_6)} e^{-k_4 t} - \frac{(k_6-k_{p2})(k_6-k_{p6})}{(k_2+k_3-k_6)(k_6-k_4)} e^{-k_6 t}, \\ Y_2(t) &= \text{Extremely complicated formula over time domain} \\ &\quad \text{(shown in Supplementary material)}, \end{aligned} \tag{11}$$

where $\otimes$ denotes the mathematical operation of convolution. The point is that we have solved the system of differential equations over the Laplace domain. In general, the solution including any external force over time domain (in this paper, C_{fd} in the C-Blood model is the external force) leads to the mathematical operation of 'convolution.' Instead, convolution over time domain corresponds to a simpler form of multiplication over the Laplace domain.

Lastly, we note that the present approach can be applied to more complex compartmental models. In compartmental models, the Laplace transformation of differential equations into algebraic equations and the following symbolic computation will reveal a rigorous relationship between kinetic constants. Furthermore, the algebraic procedure seems useful for determining constants from data.

5 Conclusion

We have derived a rigorous relationship for the kinetic constants of compartmental models for FDOPA metabolism, by symbolic computations with the aid of Gröbner bases. The algebraic procedure has successfully determined almost all constants from the observed radioactivity curves. In particular, the rigorous and simple form of a solution for the constants relationship brings us efficient parameter determination *without* blood-sampling data and *only from* PET scanning data that are dozens of minutes short of the equilibrium leading to the considerable reduction of PET scanning periods required for diagnosis.

Acknowledgment

We wish to express our gratitude to Ms. Atsuko Sono and Mr. Shigeo Orii for their supports. H. Y. and K. H. were partly supported by a Grant-in-Aid for Scientific Research on Priority Areas "Systems Genomics" (grant 18016008) from the Ministry of Education, Culture, Sports, Science and Technology of Japan. This study was supported in part by the New Energy and Industrial Technology Development Organization (NEDO) of Japan, and by The Kyushu University Research Superstar Program (SSP) from Special Coordination Funds for Promoting Science and Technology of Japan Science and Technology Agency (JST).

References

[1] Boyes, B.E., Cumming, P., Martin, W.R.W., Macgeer, E.G.: Determination of plasma [^{18}F]-6-fluorodopa during positron emission tomography: elimination and metabolism in carbidopa treated subjects. Life Sci. 39, 2243–2252 (1986)

[2] Cobelli, C., Foster, D., Toffolo, G.: Tracer Kinetics in Biomedical research: From data to model, Kluwer Academic/Plenum Publishers (2000)

[3] Cobelli, C., Toffolo, G.: Theoretical aspects and practical strategies for the identification of unidentifiable compartmental systems. In: chapter 8, pp. 85–91. Pergamon Press, Oxford (1987)

[4] Cumming, P., Gjedde, A.: Compartmental Analysis of Dopa Decarboxylation in living brain from dynamic positron emission tomograms. Synapse 29, 37–61 (1998)

[5] Deep, P., Kuwabara, H., Gjedde, A., Cumming, P.: The kinetic behaviour of [^{3}H]DOPA in living rat brain investigated by compartmental modelling of static autoradiograms. J. Neurosci. Methods 78, 157–168 (1997)

[6] Gunn, R.N., Gunn, S.R., Cunningham, V.J.: Positron emission tomography compartmental models. J. Cereb. Blood Flow Metab. 21, 635–652 (2001)

[7] Huang, S.C., Yu, D.C., Barrio, J.R., Grafton, S., Melega, W.P., Hoffman, J.M., Satyamurthy, N., Mazziotta, J.C., Phelps, M.E.: Kinetics and Modeling of L-6-[^{18}F]Fluoro-DOPA in Human Positron Emission Tomographic Studies. J. Cereb. Blood Flow Metab. 11, 898–913 (1991)

[8] Ichise, M., Ballinger, J.R., Golan, H., Vines, D., Luong, A., Tsai, S., Kung, H.F.: SPECT imaging of dopamine D2 receptors in humans with iodine 123–IBF: a practical approach to quantification not requiring blood sampling. J. Nucl. Med. 36, 11 (1995)

[9] Kawatsu, S., Kato, T., N.-Saito, A., Hatano, K., Ito, K., Ishigaki, T.: New insight into the analysis of 6-[^{18}F]fluoro-L-DOPA PET dynamic data in brain tissue without an irreversible compartment: comparative study of the Patlak and Logan Analyses. Radiation medicine 21, 47–54 (2003)

[10] Kumakura, Y., Danielsen, E.H., Reilhac, A., Gjedde, A., Cumming, P.: Levodopa effect on [^{18}F]fluorodopa influx to brain: normal volunteers and patients with Parkinson's disease. Acta Neurol. Scand. 110, 188–195 (2004), doi:10.1111/j.1600-0404.2004.00299.x

[11] Kumakura, Y., Gjedde, A., Danielsen, E.H., Christensen, S., Cumming, P.: Dopamine storage capacity in caudate and putamen of patients with early Parkinson's disease: correlation with asymmetry of motor symptoms. J. Cereb. Blood Flow Metab. 26, 358–370 (2006), doi:10.1038/sj.jcbfm.9600202

[12] Kumakura, Y., Vernaleken, I., Gründer, G., Bartenstein, P., Gjedde, A., Cumming, P.: PET studies of net blood–brain clearance of FDOPA to human brain; age–dependent decline of [^{18}F]fluorodopamine storage capacity. J. Cereb. Blood Flow Metab. 25, 807–819 (2005), doi:10.1038/sj.jcbfm.9600079

[13] Lammertsma, A.A., Bench, C.J., Hume, S.P., Osman, S., Gunn, K., Brooks, D.J., Frackowiak, R.S.J.: Comparision of methods for analysis of clinical [^{11}C]Raclopride studies. J. Cereb. Blood Flow Metab. 16, 42–52 (1996)

[14] Logan, J., Fowler, J.S., Volkow, N.D., Wang, G.-J., Ding, Y.-S., Alexoff, D.L.: Distribution Volume Ratios without blood sampling from graphical analysis of PET Data. J. Cereb. Blood Flow Metab. 16, 834–840 (1996), doi:10.1097/00004647-199609000-00008

[15] Logan, J., Fowler, J.S., Volkow, N.D., Wolf, A.P., Dewey, S.L., Schlyer, D.J., MacGregor, R.R., Hitzemann, R., Bendriem, B., Gatley, S.J., Christman, D.R.: Graphical analysis of reversible radioligand binding from time–activity measurements applied to [N-^{11}C-methyl]-(–)-Cocaine PET studies in human subjects. J. Cereb. Blood Flow Metab. 10, 740–747 (1990)

[16] Martin, W.R.W., Palmer, M.R., Patlak, C.S., Calne, D.B.: Nigrostriatal Function in Humans Studied with Positron Emission Tomography. Ann. Neurol. 26, 535–542 (1989)
[17] Melega, W.P., Hoffman, J.M., Luxen, A., Nissenson, C.H., Phelps, M.E., Barrio, J.R.: The effects of carbidopa on the metabolism of 6-[^{18}F]fluorodopa-L-DOPA in rats, monkeys and humans. Life Sci. 47, 149–157 (1990)
[18] Patlak, C.S., Blasberg, R.G.: Graphical Evaluation of Blood-to-Brain Transfer Constants from Multiple-Time uptake data. Generalizations. J. Cereb. Blood Flow Metab. 5, 584–590 (1985)
[19] Patlak, C.S., Blasberg, R.G., Fenstermacher, J.D.: Graphical evaluation of blood–to–brain transfer constants from multiple–time uptake data. J. Cereb. Blood Flow Metab. 3, 1–7 (1983)
[20] Rousset, O.G., Deep, P., Kuwabara, H., Evans, A.C., Gjedde, A.H., Cumming, P.: Effect of partial volume correction on estimates of the influx and cerebral metabolism of 6-[^{18}F]fluoro-L-dopa Studied with PET in normal control and Parkinson's Disease subjects. Synapse 37, 81–89 (2000)

Supplementary Material

Hereby, we show $Y_2(t)$, which is not shown in Eq. (11), at the following URL:
`http://www.math.kyushu-u.ac.jp/~phiroshi/pet/Y2.pdf`,
where, for instance, $Root[k_1\#1 + k_2\#1^2 + k_3\#1^3, 1]$ denotes the minimum real root of the equation $[k_1x + k_2x^2 + k_3x^3 = 0$ in x and DiracDelta[t] denotes Dirac delta function $\delta(t)$.

Appendix A: Proof of the Existence of Five Real Negative Roots

We shall prove that both $F(s)$ and $G(s)$ have five real negative roots. From Eq. (9):

$$F(s) = (s + l_1)(s + l_2)(s + l_3)F_1(s),$$
$$G(s) = (s + m_1)(s + m_2)(s + m_3)G_1(s),$$

where

$$F_1(s) = aa\, m_3(s + m_1)(s + m_2) + s(-a_2(m_2 - m_3)(s + m_1) - a_1(m_1 - m_3)(s + m_2)),$$
$$G_1(s) = bb\, l_3(s + l_1)(s + l_2) + s(-b_2(l_2 - l_3)(s + l_1) - b_1(l_1 - l_3)(s + l_2)).$$

In PET experiments, we can reasonably postulate $l_1 > l_2 > l_3 > 0$, and, $m_1 > m_2 > m_3 > 0$ because the radioactivity eventually approaches an equilibrium (the finite value). With respect to $F_1(s)$, we can see the following relationships:

$$F_1(0) = aa\, m_1m_2m_3,$$

$$F_1(-m_1) = a_1m_1(m_2 - m_1)(m_1 - m_3),\ F_1(-m_3) = -(a_1 + a_2 + aa)m_3(m_1 - m_3)(m_3 - m_2).$$

As seen in Fig. 3, $aa > 0$ because the radioactivity is never negative even when $t \to \infty$. Furthermore, the largest and the smallest time constants: $1/m_3$ and $1/m_1$ correspond to the sampling data near the equilibrium and the initial stage, respectively, leading to the coefficient relations of the exponentials, $\exp(-m_3t)$ and $\exp(-m_1t)$: $-(a_1 + a_2 + aa) > 0$ and $a_1 < 0$, respectively. These facts lead to $F_1(0) > 0$, $F_1(-m_3) < 0$ and $F_1(-m_1) > 0$, showing that $F_1(s)$ has two real negative distinct roots, and then $F(s)$ has five real negative roots. Likewise, $G(s)$ has five real negative roots. □

Appendix B: The Third-Order Polynomial in k_{b3}

In §2.4, we have derived the third-order polynomial by calculating the elimination ideal w.r.t. k_{b3}. This calculation needed 35.4 hours CPU time and 220 MBytes memory via Mathematica 5.2 (Wolfram Research, Inc.) with Intel(R) Xeon(R) CPU 2.33GHz. The calculated polynomial is as follows:

$$
\begin{aligned}
&(-r_3+r_4)(r_3-r_5)(r_4-r_5)(t_4-t_5)(t_1k_4(r_4-k_6)(r_5-k_6)k_{b3}(t_4^2(t_5-k_{b3})(t_5-k_{p2})+t_4(r_4(-(k_{b3}k_{p2})+t_5(k_{b3}+k_{p2}-k_{p6}))-(-(k_{b3}k_{p2})+t_5(k_{b3}+k_{p2}))(t_5-\\
&k_{p6}))-(r_4-t_5)k_{b3}k_{p2}(t_5-k_{p6}))(t_4^2(t_5-k_{b3})(t_5-k_{p2})+t_4(r_5(-(k_{b3}k_{p2})+t_5(k_{b3}+k_{p2}-k_{p6}))-(-(k_{b3}k_{p2})+t_5(k_{b3}+k_{p2}))(t_5-k_{p6}))-(r_5-t_5)k_{b3}\\
&k_{p2}(t_5-k_{p6}))-r_3^2(t_4(-(k_{b3}k_{p2})+t_5(k_{b3}+k_{p2}-k_{p6}))+k_{b3}k_{p2}(-t_5+k_{p6}))(-(t_1k_4(r_5-k_6)k_{b3}(t_4^2(t_5-k_{b3})(t_5-k_{p2})+t_4(r_5(-(k_{b3}k_{p2})+t_5(k_{b3}+k_{p2}\\
&-k_{p6}))-(-(k_{b3}k_{p2})+t_5(k_{b3}+k_{p2}))(t_5-k_{p6}))-(r_5-t_5)k_{b3}k_{p2}(t_5-k_{p6})))+r_4^2(t_1k_4k_{b3}(t_4(k_{b3}k_{p2}-t_5(k_{b3}+k_{p2}-k_{p6}))+k_{b3}k_{p2}(t_5-k_{p6}))+r_5^2\\
&(-(t_4^2(t_5-k_{b3})(t_5-k_{p2}))-(t_5-t_1-k_4+k_6-k_{b3})k_{b3}k_{p2}(t_5-k_{p6})+t_4(t_5^2(k_{b3}+k_{p2})+k_{b3}k_{p2}(t_1+k_4-k_6+k_{b3}+k_{p6})-t_5(-(k_6k_{b3})+k_{b3}^2-k_6k_{p2}+2k_{b3}\\
&k_{p2}+t_1(k_{b3}+k_{p2}-k_{p6})+k_4(k_{b3}+k_{p2}-k_{p6})+k_6k_{p6}+k_{p2}k_{p6})))+r_5(t_4^2k_6(t_5-k_{b3})(t_5-k_{p2})-k_{b3}(-(t_5k_6)+k_4k_{b3}+t_1(k_4+k_{b3}))k_{p2}(t_5-k_{p6})+t_4(-(t_5^2k_6(k_{b3}+k_{p2}))-k_{b3}k_{p2}(k_4k_{b3}+t_1(k_4+k_{b3})+k_6k_{p6})\\
&+t_5(k_4k_{b3}(k_{b3}+k_{p2}-k_{p6})+t_1(k_4+k_{b3})(k_{b3}+k_{p2}-k_{p6})+k_6(k_{p2}k_{p6}+k_{b3}(k_{p2}+k_{p6})))))\\
&))+r_4(t_1k_4k_{b3}(-(t_4^2(t_5-k_{b3})(t_5-k_{p2}))-(t_5+k_6)k_{b3}k_{p2}(t_5-k_{p6})+t_4(t_5^2(k_{b3}+k_{p2})+k_{b3}k_{p2}(-k_6+k_{p6})-t_5(-(k_6(k_{b3}+k_{p2}-k_{p6}))+k_{p2}k_{p6}+k_{b3}\\
&(k_{p2}+k_{p6}))))+r_5^2(t_4^2k_6(t_5-k_{b3})(t_5-k_{p2})-k_{b3}(-(t_5k_6)+k_4k_{b3}+t_1(k_4+k_{b3}))k_{p2}(t_5-k_{p6})+t_4(-(t_5^2k_6(k_{b3}+k_{p2}))-k_{b3}k_{p2}(k_4k_{b3}+t_1(k_4+k_{b3})+k_6k_{p6})\\
&+t_5(k_4k_{b3}(k_{b3}+k_{p2}-k_{p6})+t_1(k_4+k_{b3})(k_{b3}+k_{p2}-k_{p6})+k_6(k_{p2}k_{p6}+k_{b3}(k_{p2}+k_{p6}))))+r_5(t_4^2(t_5-k_{b3})(-(k_6k_{b3})+k_4(-k_6+k_{b3})+t_1(k_4-k_6+\\
&k_{b3}))(t_5-k_{p2})+k_{b3}(k_4k_6k_{b3}+t_5(-(k_6k_{b3})+k_4(-k_6+k_{b3})+t_1(k_4-k_6+k_{b3}))+t_1(k_6k_{b3}+k_4(k_6+k_{b3})))k_{p2}(t_5-k_{p6})+t_4(t_5^2(k_4(k_6-k_{b3})+k_6k_{b3}-t_1(k_4-k_6\\
&+k_{b3}))(k_{b3}+k_{p2})+k_{b3}k_{p2}(k_4k_6k_{b3}+k_4k_6k_{p6}-k_4k_{b3}k_{p6}+k_6k_{b3}k_{p6}+t_1(k_4(k_6+k_{b3}-k_{p6})-k_{b3}k_{p6}+k_6(k_{b3}+k_{p6})))-t_5(k_6k_{b3}(k_{p2}k_{p6}+k_{b3}\\
&(k_{p2}+k_{p6}))+k_4(k_6(k_{b3}^2+2k_{b3}k_{p2}+k_{p2}k_{p6})-k_{b3}(k_{p2}k_{p6}+k_{b3}(k_{p2}+k_{p6})))+t_1(k_4(k_{b3}^2+k_6(k_{b3}+k_{p2}-k_{p6})-2k_{b3}k_{p6}-k_{p2}k_{p6})+k_6(k_{b3}^2+2\\
&k_{b3}k_{p2}+k_{p2}k_{p6})-k_{b3}(k_{p2}k_{p6}+k_{b3}(k_{p2}+k_{p6}))))))))-r_3(t_1k_4(r_5-k_6)k_{b3}(t_4^2(t_5-k_{b3})(t_5-k_{p2})+t_4(r_5(-(k_{b3}k_{p2})+t_5(k_{b3}+k_{p2}-k_{p6}))-(-(k_{b3}\\
&k_{p2})+t_5(k_{b3}+k_{p2}))(t_5-k_{p6}))-(r_5-t_5)k_{b3}k_{p2}(t_5-k_{p6}))(-(t_4^2(t_5-k_{b3})(t_5-k_{p2}))-(t_5+k_6)k_{b3}k_{p2}(t_5-k_{p6})+t_4(t_5^2(k_{b3}+k_{p2})+k_{b3}k_{p2}(-k_6+k_{p6}\\
&)-t_5(-(k_6(k_{b3}+k_{p2}-k_{p6}))+k_{p2}k_{p6}+k_{b3}(k_{p2}+k_{p6}))))+r_4^2(t_4(-(k_{b3}k_{p2})+t_5(k_{b3}+k_{p2}-k_{p6}))+k_{b3}k_{p2}(-t_5+k_{p6}))(t_1k_4k_{b3}(-(t_4^2(t_5-k_{b3})(t_5\\
&-k_{p2}))-(t_5+k_6)k_{b3}k_{p2}(t_5-k_{p6})+t_4(t_5^2(k_{b3}+k_{p2})+k_{b3}k_{p2}(-k_6+k_{p6})-t_5(-(k_6(k_{b3}+k_{p2}-k_{p6}))+k_{p2}k_{p6}+k_{b3}(k_{p2}+k_{p6}))))+r_5^2(t_4^2k_6(t_5-k_{b3}\\
&)(t_5-k_{p2})-k_{b3}(-(t_5k_6)+k_4k_{b3}+t_1(k_4+k_{b3}))k_{p2}(t_5-k_{p6})+t_4(-(t_5^2k_6(k_{b3}+k_{p2}))-k_{b3}k_{p2}(k_4k_{b3}+t_1(k_4+k_{b3})+k_6k_{p6})+t_5(k_4k_{b3}(k_{b3}+k_{p2}-k_{p6}\\
&)+t_1(k_4+k_{b3})(k_{b3}+k_{p2}-k_{p6})+k_6(k_{p2}k_{p6}+k_{b3}(k_{p2}+k_{p6})))))+r_5(t_4^2(t_5-k_{b3})(-(k_6k_{b3})+k_4(-k_6+k_{b3})+t_1(k_4-k_6+k_{b3}))(t_5-k_{p2})+k_{b3}(k_4k_6k_{b3}+t_5\\
&(-(k_6k_{b3})+k_4(-k_6+k_{b3})+t_1(k_4-k_6+k_{b3}))+t_1(k_6k_{b3}+k_4(k_6+k_{b3})))k_{p2}(t_5-k_{p6})+t_4(t_5^2(k_4(k_6-k_{b3})+k_6k_{b3}-t_1(k_4-k_6+k_{b3}))(k_{b3}+k_{p2})+k_{b3}k_{p2}(k_4k_6\\
&k_{b3}+k_4k_6k_{p6}-k_4k_{b3}k_{p6}+k_6k_{b3}k_{p6}+t_1(k_4(k_6+k_{b3}-k_{p6})-k_{b3}k_{p6}+k_6(k_{b3}+k_{p6})))-t_5(k_6k_{b3}(k_{p2}k_{p6}+k_{b3}(k_{p2}+k_{p6}))+k_4(k_6(k_{b3}^2+2k_{b3}\\
&k_{p2}+k_{p2}k_{p6})-k_{b3}(k_{p2}k_{p6}+k_{b3}(k_{p2}+k_{p6})))+t_1(k_4(k_{b3}^2+k_6(k_{b3}+k_{p2}-k_{p6})-2k_{b3}k_{p6}-k_{p2}k_{p6})+k_6(k_{b3}^2+2k_{b3}k_{p2}+k_{p2}k_{p6})-k_{b3}(k_{p2}\\
&k_{p6}+k_{b3}(k_{p2}+k_{p6})))))))+r_4(-(t_1k_4k_{b3}(t_4^2(t_5-k_{b3})(t_5-k_{p2})+(t_5+k_6)k_{b3}k_{p2}(t_5-k_{p6})+t_4(-(t_5^2(k_{b3}+k_{p2}))+k_{b3}k_{p2}(k_6-k_{p6})+t_5(-(k_6(k_{b3}+k_{p2}\\
&-k_{p6}))+k_{p2}k_{p6}+k_{b3}(k_{p2}+k_{p6})))^2)+r_5^2(t_4(-(k_{b3}k_{p2})+t_5(k_{b3}+k_{p2}-k_{p6}))+k_{b3}k_{p2}(-t_5+k_{p6}))(t_4^2(t_5-k_{b3})(-(k_6k_{b3})+k_4(-k_6+k_{b3})+t_1(k_4-k_6+\\
&k_{b3}))(t_5-k_{p2})+k_{b3}(k_4k_6k_{b3}+t_5(-(k_6k_{b3})+k_4(-k_6+k_{b3})+t_1(k_4-k_6+k_{b3}))+t_1(k_6k_{b3}+k_4(k_6+k_{b3})))k_{p2}(t_5-k_{p6})+t_4(t_5^2(k_4(k_6-k_{b3})+k_6k_{b3}-t_1(k_4-\\
&k_6+k_{b3}))(k_{b3}+k_{p2})+k_{b3}k_{p2}(k_4k_6k_{b3}+k_4k_6k_{p6}-k_4k_{b3}k_{p6}+k_6k_{b3}k_{p6}+t_1(k_4(k_6+k_{b3}-k_{p6})-k_{b3}k_{p6}+k_6(k_{b3}+k_{p6})))-t_5(k_6k_{b3}(k_{p2}k_{p6}+k_{b3}\\
&(k_{p2}+k_{p6}))+k_4(k_6(k_{b3}^2+2k_{b3}k_{p2}+k_{p2}k_{p6})-k_{b3}(k_{p2}k_{p6}+k_{b3}(k_{p2}+k_{p6})))+t_1(k_4(k_{b3}^2+k_6(k_{b3}+k_{p2}-k_{p6})-2k_{b3}k_{p6}-k_{p2}k_{p6})+k_6(k_{b3}^2+\\
&2k_{b3}k_{p2}+k_{p2}k_{p6})-k_{b3}(k_{p2}k_{p6}+k_{b3}(k_{p2}+k_{p6})))))+r_5(t_4^4(t_5-k_{b3})^2((-k_4+k_6)(k_6-k_{b3})+t_1(k_4-k_6+k_{b3}))(t_5-k_{p2})^2+k_{b3}^2(t_5^2((-k_4+k_6)(k_6-k_{b3}\\
&)+t_1(k_4-k_6+k_{b3}))+k_6(k_4k_6k_{b3}+t_1(k_4k_6+2k_4k_{b3}+k_6k_{b3}))+t_5(-(k_6(k_4(k_6-k_{b3})+k_6k_{b3}))+t_1(k_6(-k_6+k_{b3})+k_4(k_6+2k_{b3})))k_{p2}^2(t_5-k_{p6})^2-t_4^3(t_5-k_{b3}\\
&)(t_5-k_{p2})(2t_5^2((-k_4+k_6)(k_6-k_{b3})+t_1(k_4-k_6+k_{b3}))(k_{b3}+k_{p2})+k_{b3}k_{p2}(t_1((k_6-k_{b3})(k_6-2k_{p6})-k_4(k_6+2k_{b3}-2k_{p6}))+k_4(k_6-k_{b3})(k_6-2k_{p6})+k_6(k_6k_{b3}\\
&+2k_6k_{p6}-2k_{b3}k_{p6}))+t_5(-(k_4(k_6-k_{b3})(k_6(k_{b3}+k_{p2}-k_{p6})-2(k_{p2}k_{p6}+k_{b3}(k_{p2}+k_{p6}))))-k_6(-2k_{b3}(k_{p2}k_{p6}+k_{b3}(k_{p2}+k_{p6}))+k_6(k_{b3}^2+2k_{p2}k_{p6}\\
&+k_{b3}(3k_{p2}+k_{p6}))+t_1(k_4(k_6(k_{b3}+k_{p2}-k_{p6})+2(k_{b3}^2-2k_{b3}k_{p6}-k_{p2}k_{p6}))-(k_6-k_{b3})(k_6(k_{b3}+k_{p2}-k_{p6})-2(k_{p2}k_{p6}+k_{b3}(k_{p2}+k_{p6}))))))+t_4k_{b3}\\
&k_{p2}(t_5-k_{p6})(-2t_5^3((-k_4+k_6)(k_6-k_{b3})+t_1(k_4-k_6+k_{b3}))(k_{b3}+k_{p2})+k_{b3}k_{p2}(k_6(k_6k_{b3}k_{p6}+k_4(2k_6k_{b3}+k_6k_{p6}-k_{b3}k_{p6}))+t_1(k_4(k_6+2k_{b3})(2k_6-k_{p6}\\
&)+k_6(2k_6k_{b3}+k_6k_{p6}-k_{b3}k_{p6}))+t_5(-(k_6k_{b3}(-2k_{b3}k_{p2}k_{p6}+k_6(3k_{p2}k_{p6}+k_{b3}(2k_{p2}+k_{p6}))))+k_4(-2k_{b3}^2k_{p2}k_{p6}-k_6^2(2k_{b3}^2+4k_{b3}k_{p2}-k_{b3}k_{p6}\\
&+k_{p2}k_{p6})+k_6k_{b3}(3k_{p2}k_{p6}+k_{b3}(2k_{p2}+k_{p6}))+t_1(-2k_{b3}^2k_{p2}k_{p6}-k_6^2(2k_{b3}^2+4k_{b3}k_{p2}-k_{b3}k_{p6}+k_{p2}k_{p6})+k_6k_{b3}(2k_{b3}k_{p2}+k_{b3}k_{p6}+3\\
&k_{p2}k_{p6})+k_4(-2k_6^2(k_{b3}+k_{p2}-k_{p6})+2k_{b3}^2(2k_{p2}+k_{p6})+k_6(-4k_{b3}^2-2k_{b3}k_{p2}+5k_{b3}k_{p6}+k_{p2}k_{p6}))))-t_5^2(-(k_4(k_6-k_{b3})(k_6(2k_{b3}+2k_{p2}-k_{p6})-2(k_{p2}\\
&k_{p6}+k_{b3}(k_{p2}+k_{p6}))))-k_6(k_6(k_{b3}+2k_{p2})(2k_{b3}+k_{p6})-2k_{b3}(k_{p2}k_{p6}+k_{b3}(k_{p2}+k_{p6})))+t_1(k_4(2(2k_{b3}+k_{p2})(k_{b3}-k_{p6})+k_6(2k_{b3}+2k_{p2}-k_{p6}))-(k_6\\
&-k_{b3})(k_6(2k_{b3}+2k_{p2}-k_{p6})-2(k_{p2}k_{p6}+k_{b3}(k_{p2}+k_{p6}))))))+t_4^2(t_5^4((-k_4+k_6)(k_6-k_{b3})+t_1(k_4-k_6+k_{b3}))(k_{b3}^2+4k_{b3}k_{p2}+k_{p2}^2)+k_{b3}^2k_{p2}^2(k_6k_{p6}
\end{aligned}
$$

$$(-(k_{b3}k_{p6})+k_6(2k_{b3}+k_{p6}))+k_4(k_{b3}k_{p6}^2-k_6k_{p6}(2k_{b3}+k_{p6})+k_6^2(k_{b3}+2k_{p6}))+t_1(k_{b3}k_{p6}^2-k_6k_{p6}(2k_{b3}+k_{p6})+k_6^2(k_{b3}+2k_{p6})+k_4(k_6^2+2k_6$$
$$(k_{b3}-k_{p6})+k_{p6}(-4k_{b3}+k_{p6})))-t_5k_{b3}k_{p2}(k_4(2k_{b3}k_{p6}(k_{p2}k_{p6}+k_{b3}(2k_{p2}+k_{p6}))+k_6^2(2k_{b3}^2+(3k_{p2}-k_{p6})k_{p6}+k_{b3}(4k_{p2}+k_{p6}))-k_6(2k_{p2}$$
$$k_{p6}^2+k_{b3}k_{p6}(7k_{p2}+k_{p6})+k_{b3}^2(2k_{p2}+3k_{p6})))+k_6(-2k_{b3}k_{p6}(k_{p2}k_{p6}+k_{b3}(2k_{p2}+k_{p6}))+k_6(2k_{p2}k_{p6}^2+k_{b3}k_{p6}(7k_{p2}+k_{p6})+k_{b3}^2(2k_{p2}+3k_{p6}$$
$$)))+t_1(2k_{b3}k_{p6}(k_{p2}k_{p6}+k_{b3}(2k_{p2}+k_{p6}))+k_6^2(2k_{b3}^2+(3k_{p2}-k_{p6})k_{p6}+k_{b3}(4k_{p2}+k_{p6}))-k_6(2k_{p2}k_{p6}^2+k_{b3}k_{p6}(7k_{p2}+k_{p6})+k_{b3}^2(2k_{p2}+3$$
$$k_{p6}))+k_4(2k_6^2(k_{b3}+k_{p2}-k_{p6})-2k_{b3}(k_{p2}-2k_{p6})k_{p6}+2k_{p2}k_{p6}^2-2k_{b3}^2(2k_{p2}+3k_{p6})+k_6(4k_{b3}^2+2k_{b3}k_{p2}-7k_{b3}k_{p6}-3k_{p2}k_{p6}+k_{p6}^2))))+t_5^3(-($$
$$k_4(k_6-k_{b3})(k_6(k_{b3}^2+3k_{b3}k_{p2}+k_{p2}^2-k_{b3}k_{p6}-k_{p2}k_{p6})-2(k_{p2}^2k_{p6}+k_{b3}^2(2k_{p2}+k_{p6})+k_{b3}k_{p2}(2k_{p2}+3k_{p6})))-k_6(k_6(k_{b3}^3+2k_{p2}^2k_{p6}+5k_{b3}$$
$$k_{p2}(k_{p2}+k_{p6})+k_{b3}^2(7k_{p2}+k_{p6}))-2k_{b3}(k_{p2}^2k_{p6}+k_{b3}^2(2k_{p2}+k_{p6})+k_{b3}k_{p2}(2k_{p2}+3k_{p6})))+t_1((-k_6+k_{b3})(k_6(k_{b3}^2+3k_{b3}k_{p2}+k_{p2}^2-k_{b3}$$
$$k_{p6}-k_{p2}k_{p6})-2(k_{p2}^2k_{p6}+k_{b3}^2(2k_{p2}+k_{p6})+k_{b3}k_{p2}(2k_{p2}+3k_{p6})))+k_4(k_6(k_{b3}^2+3k_{b3}k_{p2}+k_{p2}^2-k_{b3}k_{p6}-k_{p2}k_{p6})+2(k_{b3}^3+k_{b3}^2(k_{p2}-2$$
$$k_{p6})-k_{p2}^2k_{p6}-k_{b3}k_{p2}(k_{p2}+4k_{p6})))))+t_5^2(k_6(k_6(k_{p2}^2k_{p6}^2+k_{b3}^3(3k_{p2}+k_{p6})+k_{b3}k_{p2}k_{p6}(7k_{p2}+k_{p6})+2k_{b3}^2k_{p2}(3k_{p2}+4k_{p6}))-k_{b3}(k_{p2}^2$$
$$k_{p6}^2+2k_{b3}k_{p2}k_{p6}(3k_{p2}+k_{p6})+k_{b3}^2(3k_{p2}^2+6k_{p2}k_{p6}+k_{p6}^2)))+k_4(k_6^2(k_{b3}^3+4k_{b3}k_{p2}^2+k_{b3}^2(5k_{p2}-k_{p6})+k_{p2}(k_{p2}-k_{p6})k_{p6})-k_6(k_{p2}^2$$
$$k_{p6}^2+k_{b3}^3(3k_{p2}+k_{p6})+k_{b3}k_{p2}k_{p6}(7k_{p2}+k_{p6})+2k_{b3}^2k_{p2}(3k_{p2}+4k_{p6}))+k_{b3}(k_{p2}^2k_{p6}^2+2k_{b3}k_{p2}k_{p6}(3k_{p2}+k_{p6})+k_{b3}^2(3k_{p2}^2+6k_{p2}$$
$$k_{p6}+k_{p6}^2)))+t_1(k_6^2(k_{b3}^3+4k_{b3}k_{p2}^2+k_{b3}^2(5k_{p2}-k_{p6})+k_{p2}(k_{p2}-k_{p6})k_{p6})-k_6(k_{p2}^2k_{p6}^2+k_{b3}^3(3k_{p2}+k_{p6})+k_{b3}k_{p2}k_{p6}(7k_{p2}+k_{p6})+$$
$$2k_{b3}^2k_{p2}(3k_{p2}+4k_{p6}))+k_{b3}(k_{p2}^2k_{p6}^2+2k_{b3}k_{p2}k_{p6}(3k_{p2}+k_{p6})+k_{b3}^2(3k_{p2}^2+6k_{p2}k_{p6}+k_{p6}^2))+k_4(k_6^2(k_{b3}+k_{p2}-k_{p6})^2+k_{p2}^2k_{p6}^2+4$$
$$k_{b3}k_{p2}k_{p6}(k_{p2}+k_{p6})-2k_{b3}^3(3k_{p2}+k_{p6})+k_{b3}^2(-3k_{p2}^2+2k_{p2}k_{p6}+3k_{p6}^2)+k_6(2k_{b3}^3+k_{b3}^2(k_{p2}-5k_{p6})+k_{p2}k_{p6}(-k_{p2}+k_{p6})-k_{b3}(k_{p2}^2+6$$
$$k_{p2}k_{p6}-3k_{p6}^2)))))))))K_1/K_{p1}.$$

An Algebraic-Numeric Algorithm for the Model Selection in Kinetic Networks

Hiroshi Yoshida[1,*], Koji Nakagawa[2], Hirokazu Anai[3], and Katsuhisa Horimoto[2,*]

[1] Faculty of Mathematics, Organization for the Promotion of Advanced Research, Kyushu University, Hakozaki 6-10-1, Higashi-ku, Fukuoka 812-8581 Japan
Tel/Fax.: +81-92-642-7396
phiroshi@math.kyushu-u.ac.jp

[2] Computational Biology Research Centre (CBRC), National Institute of Advanced Industrial Science and Technology (AIST), Aomi 2-42, Koto-ku, Tokyo 135-0064, Japan
* Tel.: +81-3-3599-8711; Fax.: +81-3-3599-8081
{nakagawa-koji,k.horimoto}@aist.go.jp

[3] IT Core Laboratories, FUJITSU LABORATORIES LTD./CREST, JST., Kamikodanaka 4-1-1, Nakahara-ku, Kawasaki 211-8588, Japan
anai@jp.fujitsu.com

Abstract. We propose a novel algorithm to select a model that is consistent with the time series of observed data. In the first step, the kinetics for describing a biological phenomenon is expressed by a system of differential equations, assuming that the relationships between the variables are linear. Simultaneously, the time series of the data are numerically fitted as a series of exponentials. In the next step, both the system of differential equations with the kinetic parameters and the series of exponentials fitted to the observed data are transformed into the corresponding system of algebraic equations, by the Laplace transformation. Finally, the two systems of algebraic equations are compared by an algebraic approach. The present method estimates the model's consistency with the observed data and the determined kinetic parameters. One of the merits of the present method is that it allows a kinetic model with cyclic relationships between variables that cannot be handled by the usual approaches. The plausibility of the present method is illustrated by the actual relationships between specific leaf area, leaf nitrogen and leaf gas exchange with the corresponding simulated data.

1 Introduction

The knowledge-based approach to constructing a biological network model is recognized as one of the most promising approaches [4]. In this approach, the causal relations between biological molecules are described as a directed graph, based on the gene interaction information collected from a large number of previous reports. Since each relation identified by experimental studies is regarded as strong evidence for the existence of edges in the network model, biological network models have been constructed for various biological phenomena by a knowledge-based approach. On the other hand, it is well-known that the relationships between the molecules in a living cell change

* Corresponding authors.

V.G. Ganzha, E.W. Mayr, and E.V. Vorozhtsov (Eds.): CASC 2007, LNCS 4770, pp. 433–447, 2007.
© Springer-Verlag Berlin Heidelberg 2007

dynamically, depending on the cellular environment. Thus, the molecular relationships in the literature represent the responses to the different conditions in the experimental studies, and in the network model generated from the biological knowledge, the consistency of the model with the data observed by experimental studies must be considered carefully. Actually, several distinctive models of the relationship between molecules for a biological phenomenon can be obtained from the large amount of information in the literature [2, 5]. In these cases, a model that is consistent with the data observed under particular conditions should be selected from the candidate models.

The consistency of a model with the observed data first reminds us of the identifiability problem in the compartmental models for tracer kinetics [1, 5, 6]. In the compartmental models, the unknown parameters are estimated from tracer data in the accessible pools. The identifiability problem addresses the issue of whether the unknown parameters can be determined uniquely or non-uniquely from the tracer data. This issue has usually been solved through the transformation of differential equations into algebraic equations, by the Laplace transformation. Although a systematic algorithm for the identifiability problem was proposed [3], its application is limited to the unrealistic context of an error–free model structure and noise–free tracer data. Thus, it still seems to be difficult to solve the identifiability problem for actually observed data, in spite of the mathematical studies.

The issue of the consistency of a model with the observed data is also well known in statistics, as the test for causal hypotheses by using the observed data. The origin of the test for causal hypotheses is attributed to path analysis [12]. Unfortunately, the importance of this cornerstone research has been ignored for a long time, but the natural extension of the path analysis has been established as the well-known structural equation model (SEM) [8]. Indeed, the SEM has been utilized recently in various fields, in accordance with increased computer performance. However, the SEM without any latent variables, which is the natural form for applying the SEM to the biological networks, frequently faces difficulty in the numerical calculation of the maximum likelihood for the observed data. To overcome the difficulty of this calculation, the d-sep test [11] has been developed, based on the concept of d-separation in a directed acyclic graph [10]. Notice that the graph consistency with the data in the d-sep test can consider only the directed acyclic graph (DAG), without any cyclic relationships.

In this study, we propose a new method for selecting models, by estimating the consistency of a kinetic model with the time series of observed data. Our method is described in the following section. First, the kinetics for describing a biological phenomenon is expressed by a system of differential equations, assumed that the relationships between the variables are linear. Simultaneously, the time series of the data are numerically fitted as a series of exponentials. Next, the differential equations with the kinetic parameters and the series of exponentials fitted to the observed data are both transformed into the corresponding system of algebraic equations, by the Laplace transformation. Finally, the two systems of algebraic equations are compared by an algebraic approach. Thus, the present method estimates the model's consistency with the observed data and the determined kinetic parameters. In §3, the plausibility of the present method is illustrated by the actual relationships between specific leaf area, leaf

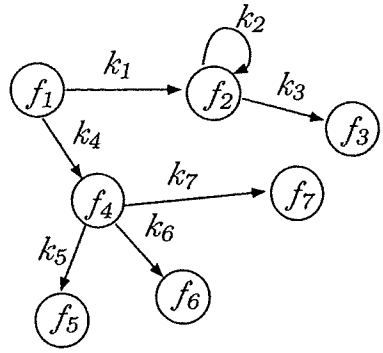

$$\Longrightarrow \begin{cases} \mathrm{d}/\mathrm{d}t\, f_1(t) = -(k_1 + k_4) f_1(t) \\ \mathrm{d}/\mathrm{d}t\, f_2(t) = k_1 f_1(t) + (k_2 - k_3) f_2(t) \\ \mathrm{d}/\mathrm{d}t\, f_3(t) = k_3 f_2(t) \\ \mathrm{d}/\mathrm{d}t\, f_4(t) = k_4 f_1(t) - (k_5 + k_6 + k_7) f_4(t) \\ \mathrm{d}/\mathrm{d}t\, f_5(t) = k_5 f_4(t) \\ \mathrm{d}/\mathrm{d}t\, f_6(t) = k_6 f_4(t) \\ \mathrm{d}/\mathrm{d}t\, f_7(t) = k_7 f_4(t) \end{cases}$$

Fig. 1. Correspondence between a network and a system of differential equations. By assuming a linear relation between the variables, the kinetics of chemicals $f_1, f_2, \ldots$ in the left graph can be described by the system of differential equations on the right side.

nitrogen and leaf gas exchange [9], with the corresponding data generated by the differential equations for the relationships. Furthermore, the merits and pitfalls of the present method are discussed. In particular, one of the merits of the present method is that it allows a kinetic model with cyclic relationships between variables that cannot be handled by the usual approaches.

2 Methods

The aim of this paper is to select the model most consistent with the given sampling data. In this section, we propose a method to perform this selection, where the model is described as a network. The network addressed in this paper designates the kinetics of chemicals, which can be described by a system of differential equations, as seen in Fig. 1.

First, we will show the overview of our method by a schematic illustration. We will then provide an explanation for the Laplace transformations of model formulae and sampling data over the time domain, as preparation for the model selection over the Laplace domain. Lastly, we describe a procedure to estimate the model consistency with the definition of *consistency measure*.

2.1 Overview

The overview of our method is schematically illustrated in Fig. 2. The point is that we perform the model selection over the Laplace domain. Therefore, both the model formulae and sampling data must be transformed into functions over the Laplace domain. Suppose that the model formulae are $\{\mathrm{d}/\mathrm{d}t\, h(t) = -k_1 h(t),\ \mathrm{d}/\mathrm{d}t\, f(t) = k_1 h(t) - k_2 f(t)\}$ and the sampling data are fitted to $h_o(t) = \beta_0 \exp(-\alpha_0 t)$, $f_o(t) = \beta_1 \exp(-\alpha_1 t) + \beta_2 \exp(-\alpha_2 t)$. The Laplace-transformed formulae of the model formula: $L[f(t)](s)$ and the fitted function: $L[fo(t)](s)$ are rational functions in s, as seen in the middle row of Fig. 2. Let *comp* denote the set of polynomials obtained by matching the coefficients in s of $L[f(t)](s)$ and $L[fo(t)](s)$ over the Laplace domain, in which every element is equal to zero when $L[f(t)](s)$ is exactly identical to $L[fo(t)](s)$ in s. Then we have adopted the smallest sum-square value of the elements in *comp* as a *consistency measure* between the model

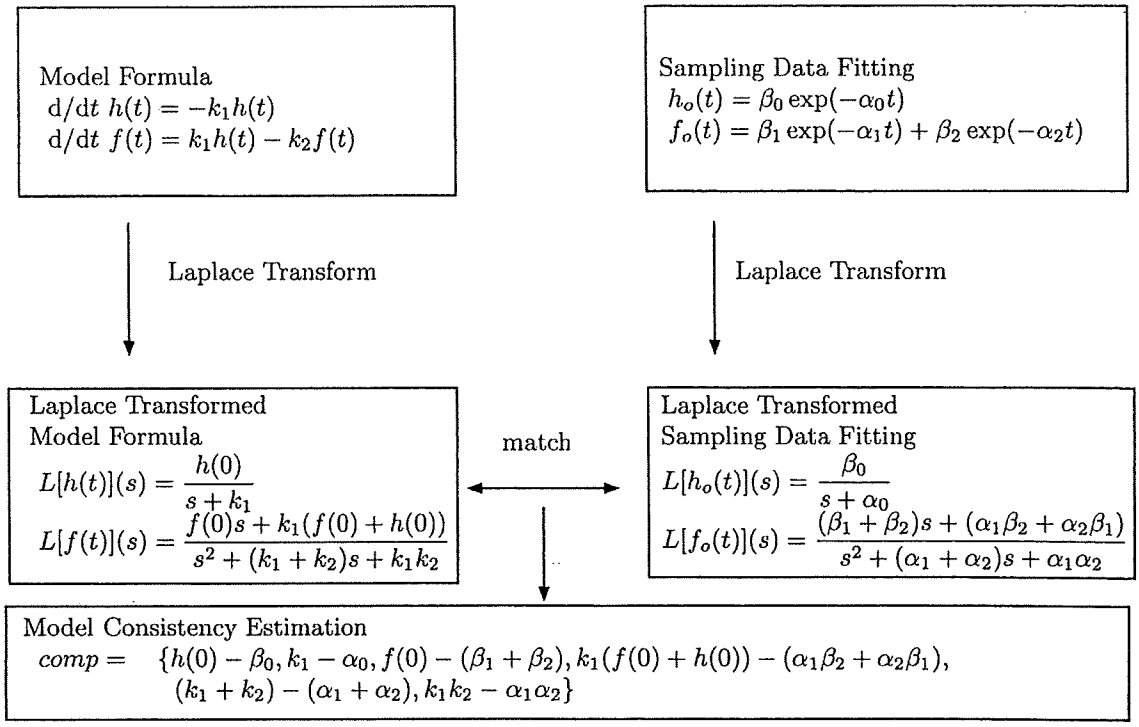

Fig. 2. Overview of our method. The top row designates the model formulae and the sampling data over the time domain, and the middle row designates their Laplace transformations. *comp* denotes the set of polynomials derived by matching the coefficients in s of $L[f(t)](s)$ and $L[fo(t)](s)$ over the Laplace domain, which is zero when the model and sampling data are completely consistent with each other.

and the sampling data, because this value is zero in the case of $L[f(t)](s) = L[fo(t)](s)$. We shall mention the formal procedure and definitions concretely in the following subsections.

2.2 Preparations: Transformation into Laplace Domain

Model Formula. Suppose that the model formulae are described over the time domain as the following system of differential equations:

$$\frac{\mathrm{d}f_i(t)}{\mathrm{d}t} = F_i(\vec{f}, \vec{k}), \tag{2.1}$$

where $\vec{f} = \{f_1, f_2, \ldots, f_n\}$ and $\vec{k} = \{k_1, k_2, \ldots, k_m\}$. $F_i(\vec{f}, \vec{k})$ can be determined in accordance with the network representing the model, and $\vec{k}$ denotes the kinetic constants between the chemicals. We transform this system of differential equations into the system of algebraic equations over the Laplace domain, and solve the equations in $L[f_i(t)](s)$ $(i = 1, 2, \ldots, n)$. Notice that in this paper, we deal only with an autonomous system of differential equations, but in the framework of the Laplace transformation, we can deal with differential equations containing external forces or 'convolutions' of complex functions, as long as the Laplace-transformed algebraic equations can explicitly be solved in $L[f_i(t)](s)$ $(i = 1, 2, \ldots, n)$.

Sampling Data Fitting. In this paper, we need the Laplace transformation of the sampling data, because we perform the model selection over the Laplace domain. Let $fo_i(t)$ denote the sampling data corresponding to $f_i(t)$ derived theoretically. By using nonlinear regression (via Maple 10 Global Optimization toolbox, ©MapleSoft), $fo_i(t)$ is expressed in terms of a series of exponentials, according to [6], as follows:

$$fo_i(t) = \beta_0 + \sum_{i=1}^{k} \beta_i \exp(-\alpha_i t), \tag{2.2}$$

where k is the number of distinct exponentials determined by $f_i(t)$, and β_0 is zero in the case of the non-existence of a constant term within $f_i(t)$. $fo_i(t)$ thus fitted is changed into the Laplace-transformed data as follows:

$$L[fo_i(t)](s) = \frac{\beta_0}{s} + \sum_{i=1}^{k} \frac{\beta_i}{s + \alpha_i}, \tag{2.3}$$

where L denotes the Laplace transformation.

2.3 Estimation of Model Consistency

Consistency Measure. To evaluate the consistency of the model with the sampling data, here we define two *consistency measures*. If the model is completely consistent with the sampling data and the data lack noise and inaccuracies, then $L[f_i(t)](s) = L[fo_i(t)](s)$ $(i = 1, 2, \ldots, n)$ holds. This fact has led us to the following definitions of consistency measure:

Let *comp* denote the set of polynomials obtained by matching the coefficients of $L[f(t)](s)$ and $L[fo(t)](s)$ over the Laplace domain, in which every element is zero in the case of $L[f_i(t)](s) = L[fo_i(t)](s)$ $(i = 1, 2, \ldots, n)$; that is, when Formula $L[f_i(t)](s) = L[fo_i(t)](s)$ is an identity in s.

The first consistency measure (in short, $CM1$) of the model is defined as the smallest sum-square value of the elements in *comp* under the following constraint:

$$k_1 > 0, k_2 > 0, \ldots, k_m > 0. \tag{2.4}$$

In order to obtain the smallest value, we have utilized the least squares method using the following equations:

$$\frac{\partial}{\partial k_1} g(\vec{k}) = 0, \frac{\partial}{\partial k_2} g(\vec{k}) = 0, \cdots, \frac{\partial}{\partial k_m} g(\vec{k}) = 0, \tag{2.5}$$

where $g(\vec{k})$ is the sum-square value of the elements in *comp*. It should be noted that in this paper we deal only with the case that the ideal associated with the set of polynomials in (2.5) is zero-dimensional. Then, we survey all of the possible candidates of the minimum by calculating *all* of the real positive roots of the system of algebraic equations (2.5). Several methods and tools exist to calculate all real roots of algebraic equations adjoined by a zero-dimensional ideal. Here we employed 'NSolve' in Mathematica 5.2 (Wolfram Research Inc.), which computes the desired roots efficiently.